Current-Split Estimation in Li-Ion Battery Pack: An Enhanced Weighted Recursive Filter Method

Haris M. Khalid, *Member, IEEE*, Qadeer Ahmed, *Member, IEEE*
Jimmy C.-H. Peng, *Member, IEEE*, and Giorgio Rizzoni, *Fellow, IEEE*

Abstract

Li-ion battery pack is a complex system consisting of numerous cells connected in parallel and series. The performance of the pack is highly dependent on the health of each individual in-pack cell. An overcharged or discharged cell connected in a parallel string could change the total capacity of the battery pack. In a pack, current-split estimation plays an important role to monitor the cell functions. Therefore, a scheme is required to estimate current-split accurately, which can thereby help to improve the overall pack performance. To what follows, a recursive weighted-covariance based estimation method (RWEM) was proposed to estimate the current-split of each set of parallel connected cells. RWEM assigns weights to the interconnected cell structure by using correlation information between battery parameters in order to estimate the current-split. This was achieved by first deriving the one-step prediction error method, where consistency for covariance was proved. Furthermore, iterative recursion for sparse measurements was also considered. Performance evaluations were conducted by analyzing sets of real-time measurements collected from Li-ion battery pack used in electric vehicles (EV). Results show that the proposed filter accurately estimated the battery parameters even in the presence of faults and random noise variances.

Index Terms

Covariance, current-split, electric vehicles (EVs), estimation, recursive, Li-ion batteries.

BMS	Battery Management System
EKF	Extended Kalman filter
EV	Electric Vehicle
KF	Kalman filter
Li-ion	Lithium ion
MSE	Mean Square Error
OSV	Open source voltage
PF	Particle filter
RWEM	Recursive weighted covariance-based estimation method
SOC	State-of-charge
UKF	Unscented Kalman filter
UPF	Unscented particle filter
$c1$	Cell 1
$c2$	Cell 2
$\mathcal{C}$	capacity of fused form of cells $c1$ and $c2$
$I_0^{\mathcal{C}}$	initial condition of the state of current
F_t	model matrix of the state response of current
α_t	temperature transition matrix of temperature
Γ_t^{c1}	temperature of Cell 1
Γ_t^{c2}	temperature of Cell 2
β_t	impedance transition matrix
z_t^{c1}	impedance of Cell 1
z_t^{c2}	impedance of Cell 2
G_t	noise transition matrix
w_t	random process noise
t	time instant
T	number of time instants
y_t	observation output of state of current
p	number of simultaneous observations for estimation
H_t	observation matrix of current state
$I_t^{\mathcal{C}}$	current state matrix
ν_t	observation noise.
R_t	residual covariance
δ_{gh}	Kronecker delta
Q_t	process noise correlation factor
I_t^{c1}	individual current of Cell $c1$
I_t^{c2}	individual current of Cell $c2$
$V_{1,t}^{\mathcal{C}}$	individual voltage of Cell $c1$
$V_{2,t}^{\mathcal{C}}$	individual voltage of Cell $c2$
$\Gamma_t^{c1^0}, \Gamma_t^{c2^0}$	room temperature for Cells $c1$ and $c2$
$z_t^{c1^0}, z_t^{c2^0}$	standard values of impedance
$R_{e,t}$	residual covariance matrix
y_t	observation output of current state
A_t^{c2}, A_t^{c2}	weighted matrices of the current-split
$P_{I,t|t}^{\mathcal{C}}$	correlation between the current estimates

I. INTRODUCTION

L I-ION batteries have become one of the preferred energy storage options in the field of EV applications. They have gained popularity because of their high energy density, light weight, and longer performance life [1]. To meet the power capacity and voltage requirements of EVs, the battery pack is composed of more than hundreds of Li-ion cells connected in-series or in-parallel.

However, each cell may exhibit variations in terms of capacity, temperature, dynamics, and aging characteristics. This may be due to adopted production technology, tolerances, material defects, and contaminations. Moreover, in actual working conditions, the temperature distribution among cells is also different due to the arrangement and position of cells. All these factors can eventually result to a lapse in uniformity between the individual cells, which may be reflected by the SOC divergence[1] or internal resistance[2] [2]. To keep the Li-ion battery system safe from these issues, BMS has been proposed at component-level [4–6] and system-level [7].

Moreover, an accurate estimation of the parameters of each battery cell can protect the battery pack from becoming overcharged or discharged, thereby extending the service life and minimizing the effects of available energy and power of a battery pack [3]. The in-pack cell with the lowest available capacity determines the overall rating of the entire pack, because it will be the first to be completely depleted during the discharging stage. Similarly, the charging of the pack will stop when the in-pack cell with the lowest available capacity is full, despite others are still not fully charged. As a result, the power capacity of the entire battery pack will be affected [8–10].

To date, many papers have been published in the literature to address the battery estimation problem in general [3, 11–24]. They can be classified into OCV-based and battery model-based methods. OCV-based methods are developed considering the difference of electrical potential between two terminals of a battery cell or pack. Popular methods are the current integral method [3], the neural network model method [11], the fuzzy logic method [12], and the support vector-based estimators [13, 14]. In the battery model-based methods, an approximate battery model is first developed using the physical laws and equations, and then an algorithm such as the KF [15, 16], EKF [17–19], UKF [20–22], PF [23] and UPF [24], are proposed to estimate the battery parame-

---

[1] SOC divergence determines the magnitude measure of the current state of the battery by analyzing the amount of sink of charge at a given point.

[2] Internal resistance of a particular source is the measure of the opposition that a circuit presents to a current when a voltage of that particular source is applied. A battery may be modeled as a voltage source in series with an internal resistance. In practice, the internal resistance of a battery is dependent on its size, chemical properties, age, temperature, and the discharge current.

ters.

Among published papers, most of the estimation schemes are developed at cell-level. Limited attention is given at pack-level. Moreover, the estimation schemes do not take into account the current-split estimation between two parallel cells connected in a series string. This is because most published methods are highly dependent on the model of the battery cell, where model equations may not consider the details about the dynamic differences between individual cells. The incomplete problem analysis can result to oversight of material contamination, variations of temperature, and conductance.

The contribution of this paper is towards enhancing the capacity estimation of the battery pack. This is accomplished by improving the observability of system parameters of each individual cell. In control theory, the observability is a measure for how well the internal states of a system can be inferred by the knowledge of its external outputs [25]. In this paper, we are trying to infer the current-split by the external outputs of total voltage and current. Also, the electromechanical dynamics of the cells are not considered here, instead, cells are considered as conducting bodies only. The information about battery as conducting bodies parameters is then extracted using a proposed filter approach named as RWEM. The proposed scheme provides a way to estimate the individual cell parameters. It is achieved by computing modal parameters from the inputs of battery system and calculating the current-split in a parallel connected cell structure. Firstly, an initial estimation of state-prediction is calculated using the prediction error innovation process using (12)–(19). It is followed by assigning weights to calculate covariance of current-split using (20)–(27). Once the current-split weighted covariance matrices are achieved, a steady-state value of fused-covariance matrix is derived for a case of ill-posed or sparse measurements in order to guarantee a feasible estimation scheme using (28)–(38). The recursive process can also calculate the other dependent battery parameters. This can be considered as a preventive maintenance strategy to replace the
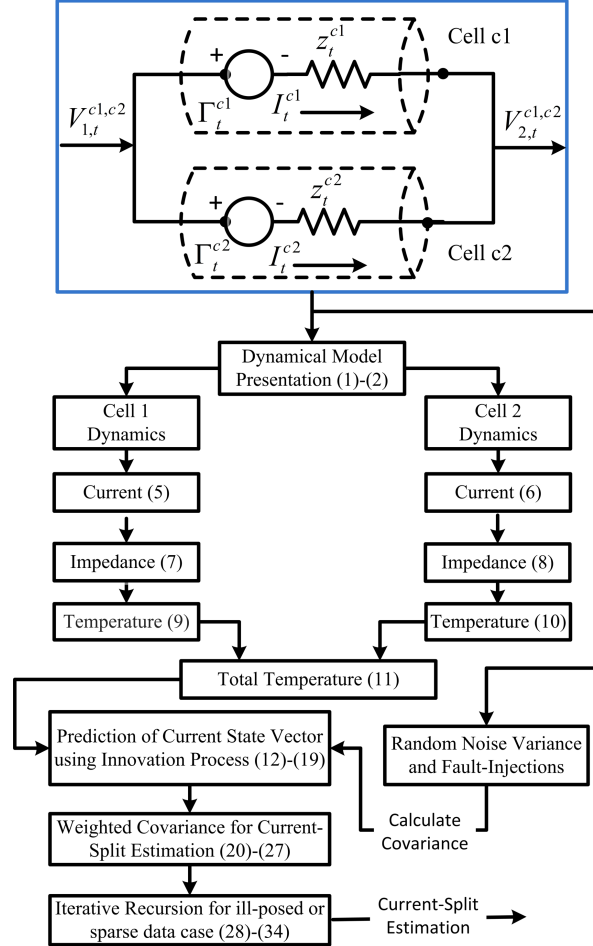
Fig. 1. Framework of RWEM for current-split estimation

effected cell in order to improve the battery pack total capacity. Note the main focus of this paper is to propose a scheme for current-split estimation in battery cells. To achieve this, we have demonstrated the effectiveness of the proposed algorithm at a constant operating environment temperature of $20^0 C$ with a single frequency. Moreover, the scheme has been tested on fresh pair of cells that have minimum manufacturing variability and aging propagation.

The paper is organized as follows: The problem is formulated in Section II. In Section III, the implementation and evaluation of the scheme are discussed, and finally conclusions are drawn in Section IV.

5

II. PROBLEM FORMULATION

The formulation begins with outlining the assumed system model, followed by the state representation of battery parameters. The RWEM algorithm is then built on it for calculating the current-split estimates. An overview of the formulation framework of this section is illustrated in Fig. 1. It summarizes the formulation and equations involved at each step while estimating the current-split and other parameters of the battery-pack. Note that only two parallel cells connected in a thread of series are considered here. This is the standard structure used in Li-ion battery packs [26].

A. State Formulation with Observation Model

Consider a discrete-time dynamical model of a battery-pack at a time $t + 1$ evolved from its prior state at time t. Two cells connected in parallel with a voltage supply in-series are expressed as:

$$
\begin{aligned}
I_{t+1}^{\mathcal{C}} &= F_t I_t^{\mathcal{C}} + \frac{\alpha_t}{2}(\Gamma_t^{c1} + \Gamma_t^{c2}) + \beta_t(z_t^{c1} + z_t^{c2}) \\
&\quad + G_t w_t, \ t = 0, 1, ..., T
\end{aligned}
\tag{1}
$$

where the superscripts $c1$ and $c2$ denote Cell 1 and Cell 2, respectively. The symbol $\mathcal{C}$ is used to present the capacity of fused form of cells $c1$ and $c2$, i.e. $\mathcal{C} = c1 + c2$, whereas $\mathcal{C}'$ presents the transpose of this fused form. The $I_0^{\mathcal{C}} \in \mathbf{R}^r$ is the initial condition of the state of current, $F_t \in \mathbf{R}^{r \times r}$ is a model matrix of the state response of current, such that it depends on covariates, $\alpha_t \in \mathbf{R}^{r \times r}$ is the temperature transition matrix of temperature $\Gamma_t^{c1} \in \mathbf{R}^r$ and $\Gamma_t^{c2} \in \mathbf{R}^r$ of Cell 1 and Cell 2 respectively. Also, $\beta_t \in \mathbf{R}^{r \times r}$ is the impedance transition matrix of impedances $z_t^{c1} \in \mathbf{R}^r$ and $z_t^{c2} \in \mathbf{R}^r$ respectively. $G_t \in \mathbf{R}^{r \times r}$ is the noise transition matrix, which can be defined as a probability vector whose elements are non-negative real numbers and sum to 1. $w_t \in \mathbf{R}^r$ is the random process noise, t is the time instant, and T refers to the number of time instants. Let the battery-pack,

6

described in (1), be observed at time-instant t as:

$$y_t = H_t F_t I_t^{\mathcal{C}} + \nu_t \tag{2}$$

where $y_t \in \mathbf{R}^p$ is the observation output of state of current, p is the number of simultaneous observations for estimation made at time instant t, $H_t \in \mathbf{R}^{p \times r}$ is the observation matrix of current state, $I_t^{\mathcal{C}}$ is the current state matrix, and $\nu_t \in \mathbf{R}^p$ is the observation noise.

It has been initially assumed that the noises w_t and ν_t are uncorrelated, and are zero-mean white noise sequences with Gaussian distribution:

$$\mathbf{E}[w_t] = \mathbf{E}[\nu_t] = \mathbf{E}[w_g \nu_h'] = 0, \, \forall \, t \tag{3}$$

$$\mathbf{E}[w_g w_h'] = R_t \delta_{gh}, \, \mathbf{E}[\nu_g \nu_h'] = Q_t \delta_{gh}, \, \forall \, t \tag{4}$$

Note R_t represents the residual covariance, δ_{gh} is a Kronecker delta which is one when variables g and h are the same. Q_t is the process noise correlation factor, and superscript $'$ represents the transpose.

B. Relationship Between Battery Parameters

Once the observation model is extracted from the measurements of the battery pack, the relation between different parameters of the battery are formulated. Note the known parameters of parallel cells connected in a series string are the string voltages, temperatures and current.

At time instant t, I_t^{c1} is the individual current of Cell $c1$, and can be represented as the difference between voltage $V_{1,t}^{\mathcal{C}}$ and $V_{2,t}^{\mathcal{C}}$ as:

$$I_t^{c1} = \frac{V_{1,t}^{\mathcal{C}} - V_{2,t}^{\mathcal{C}}}{z_t^{c1}} \tag{5}$$

Similarly, I_t^{c2} is the individual current of Cell $c2$, and is defined as:

$$I_t^{c2} = \frac{V_{1,t}^{\mathcal{C}} - V_{2,t}^{\mathcal{C}}}{z_t^{c2}} \tag{6}$$

Also, impedances z_t^{c1} and z_t^{c2} for cells $c1$ and $c2$ are:

$$z_t^{c1} = z_t^{c1^0} + \left[1 + \alpha_t(\Gamma_t^{c1} - \Gamma_t^{c1^0})\right], \tag{7}$$

$$z_t^{c2} = z_t^{c2^0} + \left[1 + \alpha_t(\Gamma_t^{c2} - \Gamma_t^{c2^0})\right] \tag{8}$$

Note in (7)–(8), the standard relation between impedance and temperature is considered for Cell $c1$ and $c2$ according to [27]. Here $z_t^{c1^0}$ and $z_t^{c2^0}$ are the standard values of impedance at room temperature $\Gamma_t^{c1^0}$ and $\Gamma_t^{c2^0}$ respectively. α_t is the transition matrix of temperature. (7) can be expressed for temperature Γ_t^{c1} of Cell 1 as:

$$\Gamma_t^{c1} = \frac{z_t^{c1}}{\alpha z_t^{c1^0}} - \frac{1}{\alpha} + \Gamma_t^{c1^0} \tag{9}$$

Similarly, temperature $\Gamma_{c2,t}$ of Cell 2 is:

$$\Gamma_t^{c2} = \frac{z_t^{c2}}{\alpha z_t^{c2^0}} - \frac{1}{\alpha} + \Gamma_t^{c2^0} \tag{10}$$

Since $\Gamma_t^{\mathcal{C}} = \frac{\Gamma_t^{c1} + \Gamma_t^{c2}}{2}$,

$$\begin{aligned}
\Gamma_t^{\mathcal{C}} &= \frac{z_t^{c1}}{2\alpha_t z_t^{c1^0}} + \frac{z_t^{c2}}{2\alpha_t z_t^{c2^0}} + \frac{\Gamma_t^{c1^0}}{2} + \frac{\Gamma_t^{c2^0}}{2} - \frac{1}{\alpha_t} \\
&= \frac{z_t^{c1} z_t^{c2^0} + z_t^{c2} z_t^{c1^0} - 2 z_t^{c1^0} z_t^{c2^0}}{2\alpha_t z_t^{c1^0} z_t^{c2^0}} \\
&\quad + \frac{\alpha_t \Gamma_t^{c1^0} z_t^{c1^0} z_t^{c2^0} + \alpha_t \Gamma_t^{c2^0} z_t^{c1^0} z_t^{c2^0}}{\alpha_t z_t^{c1^0} z_t^{c2^0}}
\end{aligned} \tag{11}$$

Thus, the general relation between battery parameters is developed.

To find the current-split estimation, the individual state of current $I_t^{\mathcal{C}}$ needs to be determined. Note that each Li-ion cell has a nominal voltage of 3.2 V. Hence, any variations will be occurring in a bounded-capacity, which requires a good initial parameter value estimate. It is particularly true for this paper as no battery-model is used. Good initial parameter values can provide a good estimate and improve the ability to predict the dependent battery parameters expressed in (5) to (11). To achieve this, an uncorrelated innovation process is used to develop confidence intervals around the prediction profile of the current-split. It is to ensure the best possible approximation of

the true system even when the battery model is not available.

C. Prediction of State Vector of Current using by Innovation Process

Given the uncorrelated innovation process, the recursive one-step prediction estimate of $I_t^{\mathcal{C}}$ can be presented as:

$$\hat{I}_{t+1}^{\mathcal{C}} = (\mathbf{E}[I_T^{\mathcal{C}}])R_{e,t-1}^{\mathcal{C}^{-1}}e_{t-1}$$

$$\hat{I}_{t+1}^{\mathcal{C}} = \sum_{t-1}^{t+1}(I_{t+1}^{\mathcal{C}}, e_{t-1})R_{e,t-1}^{\mathcal{C}^{-1}}e_{t-1} \tag{12}$$

where $R_{e,t}$ is the residual covariance matrix of the difference between the observation output of current state y_t and its estimate $\hat{y}_t$, denoted by $e_t = y_t - H_t\hat{I}_{t|t-1}^{\mathcal{C}}$. Accordingly, the state of current can be computed from the most recent past value $\hat{I}_{t|t-1}^{\mathcal{C}}$ and the new information in e. A more indicative form of recursion of (12) is:

$$\hat{I}_{t+1|t}^{\mathcal{C}} = \left[\sum_{t=0}^{t+1}(I_{t+1}^{\mathcal{C}}, e_{t-1})R_{e,t-1}^{c1^{-1}}e_{t-1}\right] + (I_{t+1}^{\mathcal{C}}, e_t)R_{e,t}^{c2^{-1}}e_t \tag{13}$$

where $\left[\sum_{t=0}^{t+1}(I_{t+1}^{\mathcal{C}}, e_{t-1})R_{e,t-1}^{c1^{-1}}e_{t-1}\right]$ is the estimate of the one-step prediction. Therefore,

$$\hat{I}_{t+1|t}^{\mathcal{C}} = \hat{I}_{t+1|t-1}^{\mathcal{C}} + (I_{t+1}^{\mathcal{C}}, e_{t-1})R_{e,t-1}^{-1}(y_t - H_t\hat{I}_{t|t-1}^{\mathcal{C}}) \tag{14}$$

which completes the one-step prediction for the state of current, $I_t^{\mathcal{C}}$. Considering the difference between $I_t^{\mathcal{C}}$ and its estimate $\hat{I}_t^{\mathcal{C}}$ as $\tilde{I}_{t|t}^{\mathcal{C}}$, the initial condition of the state of current is:

$$\tilde{I}_{0|0}^{\mathcal{C}} = I_{0|0}^{\mathcal{C}} - \hat{I}_{0|0}^{\mathcal{C}}$$

$$= F_0 I_{0|0}^{\mathcal{C}} + \alpha_0(\Gamma_{0|0}^{c1} + \Gamma_{0|0}^{c2}) + \beta_0(z_{0|0}^{c1} + z_{0|0}^{c2}) + G_1 w_1$$

$$- F_0\hat{I}_{0|0}^{\mathcal{C}} - (I_{t+1}^{\mathcal{C}}, e_t)R_{e,t}^{-1}\Big[H_t(F_0 I_{0|0}^{\mathcal{C}} + \alpha_0(\Gamma_{0|0}^{c1}$$

$$+ \Gamma_{0|0}^{c2}) + \beta_0(z_{0|0}^{c1} + z_{0|0}^{c2}) + G_1 w_1) + \nu_1 - H_1 F_0\hat{I}_0^{\mathcal{C}}\Big] \tag{15}$$

Rearranging (15) gives,

$$\tilde{I}_{0|0}^{\mathcal{C}} = \Big[1 - (I_{0|0}^{\mathcal{C}}, e_1)R_{e,1}^{-1}H_1\Big]F_0\tilde{I}_{0|0}^{\mathcal{C}} + \Big[1 - (I_0^{\mathcal{C}}, e_1)R_{e,1}^{-1}H_1\Big]$$

$$G_1 w_1 - \Big[1 - (I_0^{\mathcal{C}}, e_1)R_{e,1}^{-1}H_1\Big]F_0 I_{0|0}^{\mathcal{C}} + \Big[1 - (I_0^{\mathcal{C}}, e_1)$$

$$R_{e,1}^{-1}H_1\Big]\Big[\alpha_0\Gamma_0^{c1}+\alpha_0\Gamma_0^{c2}\Big]+\Big[1-(I_0^{\mathcal{C}},e_1)R_{e,1}^{-1}H_1\Big]$$

$$\Big[\beta z_{0|0}^{c1}+\beta z_{0|0}^{c2}\Big]-(I_{0|0}^{\mathcal{C}},e_1)R_{e,1}^{-1}\nu_1 \tag{16}$$

Hence, the covariance matrix for current difference of Cell 1 and Cell 2 is:

$$P_{I,1|1}^{\mathcal{C}}=\mathbf{E}[\tilde{I}_{1|1}^{c1}\tilde{I}_{1|1}^{c2'}]=\Big[1-(I_{1|1}^{c1},e_{1|1})R_{e,1|1}^{c1^{-1}}\Big]Q_0\Big[1-(I_{1|1}^{c2},e_{1|1})$$

$$R_{e,1|1}^{-1}\Big]'+\Big[1-(I_{0|0}^{\mathcal{C}},e,1|1)R_{e,1|1}^{-1}\Big]F_0 I_0^{\mathcal{C}}+\Big[1-(I_0^{\mathcal{C}},e_1)R_{e,1}^{-1}H_1\Big]$$

$$\Big[\beta z_{0|0}^{c1}+\beta z_{0|0}^{c2}\Big]-(I_{0|0}^{\mathcal{C}},e_1)R_{e,1}^{-1}\nu_1 \tag{17}$$

Similar to (17), the fused difference of $\tilde{I}_{t|t}^{\mathcal{C}}$ can be written as:

$$\tilde{I}_{t|t}^{\mathcal{C}}=\Big[1-(I_{t|t}^{\mathcal{C}},e_{t-1})R_{e,t-1}^{-1}H_t\Big]F_t\tilde{I}_{t|t}^{\mathcal{C}}+\Big[1-(I_t^{\mathcal{C}},$$

$$e_{t-1})R_{e,t-1}^{-1}H_t\Big]G_t w_t-\Big[1-(I_t^{\mathcal{C}},e_t)R_{e,t}^{-1}H_t\Big]F_t$$

$$I_{t|t}^{\mathcal{C}}+\Big[1-(I_t^{\mathcal{C}},e_t)R_{e,t}^{-1}H_t\Big]\Big[\alpha_t\Gamma_t^{c1}+\alpha_t\Gamma_t^{c2}\Big]+\Big[1-$$

$$(I_t^{\mathcal{C}},e_t)z_{t|t}^{c1}R_{e,t}^{-1}H_t\Big]\Big[\beta+\beta z_{t|t}^{c2}\Big]-(I_{t|t}^{\mathcal{C}},e_t)R_{e,t}^{-1}\nu_t \tag{18}$$

which yields the covariance matrix for the fused difference of current $\tilde{I}_{t|t}^{\mathcal{C}}$ as:

$$P_{I,t|t}^{\mathcal{C}}=\Big[1-(I_{t+1}^{c1},e_t)R_{e,t-1}^{c1^{-1}}H_t^{c1}\Big]F_{t-1}P_{t-1|t-1}^{\mathcal{C}}F_{t-1}'$$

$$\Big[1-(I_{t+1}^{c2},e_t)R_{e,t-1}^{c2^{-1}}H_t^{c2}\Big]F_{t-1}'+\Big[1-(I_{t+1}^{c2},e_t)$$

$$R_{e,t-1}^{c2^{-1}}H_t^{c2}\Big]'+\Big[1-(I_t^{\mathcal{C}},e_t)R_{e,t-1}^{-1}H_t\Big]\Big[\alpha\Gamma_t^{c1}$$

$$+\alpha\Gamma_t^{c2}\Big]+\Big[1-(I_t^{\mathcal{C}},e_t)R_{e,t-1}^{-1}H_t\Big]\Big[\beta z_{t|t}^{c1}+\beta z_{t|t}^{c2}\Big] \tag{19}$$

The initialization of the current states I_t^{c1} and I_t^{c2} was made using the innovation process. However, the derived covariance matrix assumes that both cells have the same impedance, operating temperature, and other cell dynamics. This leads to the motivation to consider the problem for battery pack with dynamic in-cell variations. Variations in the individual cells are primarily due to cell total capacity, internal resistance, and the initial value of SOC, which gives the reason to derive a covariance matrix that can represent the dynamical situation of current-split estimation.

The proposed solution is to assign weights to the states of current, I_t^{c1} and I_t^{c2}, and calculate a weighted covariance of current-split with recursion.

D. *Weighted Covariance for Estimation of Current-Split*

The recursive estimate of the current-split can be represented as a sum of weights:

$$\hat{I}_{t|t}^{\mathcal{C}} = A_t^{c1}\hat{I}_t^{c1} + A_t^{c2}\hat{I}_t^{c2} \tag{20}$$

where A_t^{c2} and A_t^{c2} are the weighted matrices of the current-split. Therefore, the difference between $\hat{I}_t^{c1}$ and $\hat{I}_t^{c2}$ can be expressed by $\delta_t^{\mathcal{C}}$ as follows:

$$\delta_t^{\mathcal{C}} = \hat{I}_{t|t}^{c1} - \hat{I}_{t|t}^{c2} \tag{21}$$

The expression (21) can be normalized further as:

$$\mathbf{E}[\delta_t^{\mathcal{C}}\delta_t^{\mathcal{C}'}] = \mathbf{E}[\hat{I}_{t|t}^{c1} - I_{t|t}^{\mathcal{C}} - (\hat{I}_{t|t}^{c2} - I_{t|t}^{\mathcal{C}})][\hat{I}_{t|t}^{c1}$$
$$- I_{t|t}^{\mathcal{C}} - (\hat{I}_{t|t}^{c2} - I_{t|t}^{\mathcal{C}})]' \tag{22}$$

and is equivalent to:

$$\mathbf{E}[\delta_t^{\mathcal{C}}\delta_t^{\mathcal{C}'}] = P_{I,t|t}^{c1} + P_{I,t|t}^{c2} - P_{I,t|t}^{\mathcal{C}} - P_{I,t|t}^{\mathcal{C}'} \tag{23}$$

The term $P_{I,t|t}^{\mathcal{C}}$ refers to the associated covariance of fused current with its estimate $\hat{I}_{t|t}^{\mathcal{C}}$. Also,

$$P_{I,t|t}^{\mathcal{C}} = \mathbf{E}[(\hat{I}_{t|t}^{c1} - I_t^{\mathcal{C}})(\hat{I}_{t|t}^{c2} - I_t^{\mathcal{C}})'] = \mathbf{E}[\tilde{I}_{t|t}^{c1}\tilde{I}_{t|t}^{c2}] = P_{I,t|t}^{\mathcal{C}'} \tag{24}$$

where $P_{I,t|t}^{\mathcal{C}}$ is the correlation between the two current estimates $\hat{I}_t^{c1}$ and $\hat{I}_t^{c2}$, respectively. Using the calculation from (12)–(19), the weighted matrix of the current-split for I_t^{c1} can be expressed as:

$$A_t^{c1} = \left(P_{I,t|t}^{c2} - P_{I,t|t}^{\mathcal{C}'}\right)\left(P_{I,t|t}^{c1} + P_{I,t|t}^{c2} - P_{I,t|t}^{\mathcal{C}} - P_{I,t|t}^{\mathcal{C}'}\right)^{-1} \tag{25}$$

Similarly, the weighted matrix for current-split of I_t^{c2} is:

$$A_t^{c2} = \left(P_{I,t|t}^{c1} - P_{t|t}^{\mathcal{C}}\right)\left(P_{I,t|t}^{c1} + P_{I,t|t}^{c2} - P_{I,t|t}^{\mathcal{C}} - P_{I,t|t}^{\mathcal{C}'}\right)^{-1} \tag{26}$$

Considering (25) and (26), the covariance matrix for the fused current-split is:

$$P_{I,t|t}^{\mathcal{C}} = P_{I,t|t-1}^{\mathcal{C}} - \left(P_{I,t|t}^{c2} - P_{I,t|t}^{\mathcal{C}'} \right) \left(P_{I,t|t}^{c1} + P_{I,t|t}^{c2} \right.$$
$$\left. - P_{I,t|t}^{\mathcal{C}} - P_{I,t|t}^{\mathcal{C}'} \right)^{-1} \left(P_{I,t|t}^{c2} - P_{I,t|t}^{\mathcal{C}'} \right)' \tag{27}$$

The weights have also been defined in a closed-form in (25) and (26). Note, the covariance matrices of temperature and voltage can also be calculated by using (5)–(11). In order to satisfy convergence for the estimator, the fused covariance matrix for the current-split requires a proof of consistency, which is shown in the Appendix. ■

However, the current-split information from each individual cell and its respective covariance matrix are highly dependent on the difference of in-series voltages and the relation between temperature and impedance as noted in (5)–(11). There can be a condition where the current-split estimation is an ill-posed or sparse problem. This is the case when one of the cells is generating random zero values, which will make the solution of (25) and (26) infeasible because of the inverse matrix and closed-form solution. In order to guarantee a feasible estimation, an iterative method is required to develop which can generate a feasible solution for an ill-posed or sparse data condition.

E. Current-Split Estimation during an Ill-Posed Condition

In this section, a recursive loop is built on top of (20)–(27) to give feedback to the updated current estimate and its associated covariance at each time-instant. The implicit fused current estimate can be expressed as:

$$\hat{I}_{t|t}^{\mathcal{C}} = P_{I,t|t}^{\mathcal{C}} \left[P_{I,t|t}^{c2} F_t \hat{I}_{t|t-1}^{\mathcal{C}} + (P_{I,t|t}^{c2} - P_{I,t|t}^{\mathcal{C}'})(P_{I,t|t}^{c1} \right.$$
$$\left. + P_{I,t|t}^{c2} - P_{I,t|t}^{\mathcal{C}} - P_{I,t|t}^{\mathcal{C}'})^{-1}(P_{I,t|t}^{c2} - P_{I,t|t}^{\mathcal{C}'})' \right]^{-1}$$
$$P_{I,t|t}^{\mathcal{C}'}(A_t^{c1} F_t \hat{I}_{t|t}^{c1} + A_{t|t}^{c2} F_t \hat{I}_{t|t}^{c2}) \tag{28}$$

It can be simplified as:

$$\hat{I}_{t|t}^{\mathcal{C}} = A_T^{c1} P_{I,t|t}^{\mathcal{C}} A_t^{c1} F_t I_{t|t}^{c1} + A_T^{c2} P_{I,t|t}^{\mathcal{C}} A_t^{c2} F_t I_{t|t}^{c2} \tag{29}$$

where, A_T^{c1} and A_T^{c2} are the identity matrices, $A_t^{c1} = A_{t-1}^{c1} P_{I,t|t}^{\mathcal{C}} \left[P_{I,t|t}^{c2} F_t \hat{I}_{t|t-1}^{\mathcal{C}} + (P_{I,t|t}^{c2} - P_{I,t|t}^{\mathcal{C}'})(P_{I,t|t}^{c1} + P_{I,t|t}^{c2} - P_{I,t|t}^{\mathcal{C}} - P_{I,t|t}^{\mathcal{C}'})^{-1}(P_{I,t|t}^{c2} - P_{I,t|t}^{\mathcal{C}'})' \right]^{-1}$. Also, $A_t^{c2} = A_{t-1}^{c2} P_{t|t}^{\mathcal{C}} \left[P_{I,t|t}^{c1} F_t \hat{I}_{t|t-1}^{\mathcal{C}} + (P_{I,t|t}^{c1} - P_{I,t|t}^{\mathcal{C}'})(P_{I,t|t}^{c2} + P_{I,t|t}^{c1} - P_{I,t|t}^{\mathcal{C}} - P_{I,t|t}^{\mathcal{C}'})^{-1}(P_{I,t|t}^{c1} - P_{I,t|t}^{\mathcal{C}'})' \right]^{-1}$. Considering the feedback of the estimate, and computing with the inverse of the covariance matrix gives:

$$
\begin{aligned}
P_{I,t|t}^{\mathcal{C}^{-1}} \hat{I}_{t|t}^{\mathcal{C}} = & -(N-1) P_{I,t|t-1}^{\mathcal{C}^{-1}} \hat{I}_{t|t-1}^{\mathcal{C}} + \Big[P_{I,t|t}^{c2} - (P_{I,t|t}^{c2} \\
& - P_{I,t|t}^{\mathcal{C}'})(P_{I,t|t}^{c1} + P_{I,t|t}^{c2} - P_{I,t|t}^{\mathcal{C}} - P_{I,t|t}^{\mathcal{C}'})^{-1}(P_{I,t|t}^{c2} \\
& - P_{I,t|t}^{\mathcal{C}'})' \Big]^{-1} (A_t^{c1} \hat{I}_{t|t}^{c1} + A_t^{c2} \hat{I}_{t|t}^{c2})
\end{aligned}
\tag{30}
$$

where N is the number of cells, which is 2 for this formulation. To compute the steady state error covariance of fused current state estimate $I_{t|t}^{\mathcal{C}}$, subtracting $P_{t|t}^{\mathcal{C}^{-1}}$ from both sides of (30) and substituting (29) yields:

$$
\begin{aligned}
& P_{I,t|t}^{\mathcal{C}^{-1}} (\hat{I}_{t|t}^{\mathcal{C}} - I_t^{\mathcal{C}}) = \\
& -P_{I,t|t}^{\mathcal{C}^{-1}} I_t^{\mathcal{C}} - (N-1) P_{I,t|t-1}^{\mathcal{C}^{-1}} \hat{I}_{t|t-1}^{\mathcal{C}} - (N-1) P_{I,t|t-1}^{\mathcal{C}^{-1}} \\
& \hat{I}_{t|t-1}^{\mathcal{C}} + \Big[P_{I,t|t}^{c2} - (P_{t|t}^{c2} - P_{I,t|t}^{\mathcal{C}'})(P_{I,t|t}^{c1} + P_{t|t}^{c2} - P_{I,t|t}^{\mathcal{C}} - P_{I,t|t}^{\mathcal{C}'})^{-1} \\
& (P_{I,t|t}^{c2} - \Sigma_{t|t}^{\mathcal{C}'})^T \Big]^{-1} (A_t^{c1} \hat{I}_{t|t}^{c1} + A_t^{c2} \hat{I}_{t|t}^{c2})
\end{aligned}
\tag{31}
$$

Rearranging (31) gives:

$$
\begin{aligned}
= & -(N-1) P_{I,t|t-1}^{\mathcal{C}^{-1}} F_{t-1} (\hat{I}_{t-1|t-1}^{\mathcal{C}} - I_{t-1}^{\mathcal{C}}) - P_{I,t|t}^{\mathcal{C}^{-1}} I_t^{\mathcal{C}} \\
& -(N-1) P_{I,t|t-1}^{\mathcal{C}^{-1}} F_{t-1} I_{t-1}^{\mathcal{C}} + P_{I,t|t}^{\mathcal{C}^{-1}} \Big[A_{t-1} P_{I,t|t}^{\mathcal{C}} A_t^{c1} F_t I_{t|t}^{c1} \\
& + A_{t-1} P_{I,t|t}^{\mathcal{C}} A_t^{c2} F_t \hat{I}_{t|t}^{c2} \Big]
\end{aligned}
\tag{32}
$$

Through simple algebra manipulations and substituting (2), we can re-write (31) as

$$
\begin{aligned}
& P_{I,t|t}^{\mathcal{C}^{-1}} (\hat{I}_{t|t}^{\mathcal{C}} - I_t^{\mathcal{C}}) = \\
& \Big[-(N-1) P_{I,t|t-1}^{\mathcal{C}^{-1}} F_t + P_{t|t}^{\mathcal{C}^{-1}} A_{t-1} P_{I,t|t}^{\mathcal{C}} A_t^{c1} F_t + P_{I,t|t}^{\mathcal{C}^{-1}} \\
& A_t P_{I,t|t}^{\mathcal{C}} A_t^{c2} F_t \Big] (\hat{I}_{t-1|t-1}^{\mathcal{C}} - \hat{I}_{t|t}^{c1} - \hat{I}_{t|t}^{c2}) + P_{I,t|t}^{\mathcal{C}^{-1}} A_{t-1} P_{I,t|t}^{\mathcal{C}} A_t^{c1}
\end{aligned}
$$

$$F_t \hat{I}_{t-1}^{c1} + P_{I,t|t}^{\mathcal{C}^{-1}} A_{t-1} P_{I,t|t}^{\mathcal{C}} A_t^{c2} F_t \hat{I}_{t|t-1}^{c2} - P_{I,t|t}^{\mathcal{C}^{-1}} I_t^{\mathcal{C}}$$

$$- (N-1) P_{I,t|t-1}^{\mathcal{C}^{-1}} F_{t-1} I_{t-1}^{\mathcal{C}} \tag{33}$$

which develops a recursive loop in order to guarantee feasible solution for the estimator. Furthermore, in order to verify stability, (33) can be written in the form of a discrete Lyapunov equation. This can be seen in the Appendix. ∎

III. IMPLEMENTATION AND EVALUATION

The proposed estimation scheme was exhaustively assessed on Li-ion battery-pack under different operating conditions. The experiments were carried out at the battery laboratory in the Center for Automotive Research (CAR) [28] according to the guidelines issued by United States Department of Energy battery test manual [29, 30]. Three of the studies are presented in this paper. Each study presents a structure of cells connected in parallel in a series thread as shown in Fig. 2. Test Case I analyzed the nominal values collected from the parallel structure of cells in Fig. 2(a). The proposed method is referenced with two main stream techniques: 1) Extended Kalman filter [31, 32], and 2) Unscented Kalman filter [33]. Test Case II examined the cell structure shown in Fig. 2(b) with random noise variance. This was followed by Test Case III, which considered a current-split estimation in the presence of injected fault. Note the implementation was preferred to test offline because of two main reasons: Firstly, a fault injection can be detected by a BMS. This detection may result in system shut-off or a compensation of the fault. Secondly, if the BMS is unavailable to detect the fault, the injected fault may result in potential damage to battery. Therefore, to be able to cover the whole set of considered faults in a consistent way, the off-line approach has been chosen. In all three test cases, the characterized battery cell is a cylindrical A123 ANR26650 Li-ion iron-phosphate ($LiFePO_4$) cell with a nominal capacity of 2.3 Ah and a nominal voltage of 3.2 V. The experimental setup is composed of 800W programmable electronic load, 1.2 kW programmable power supply, a data acquisition unit for collecting measurement signals, a thermal
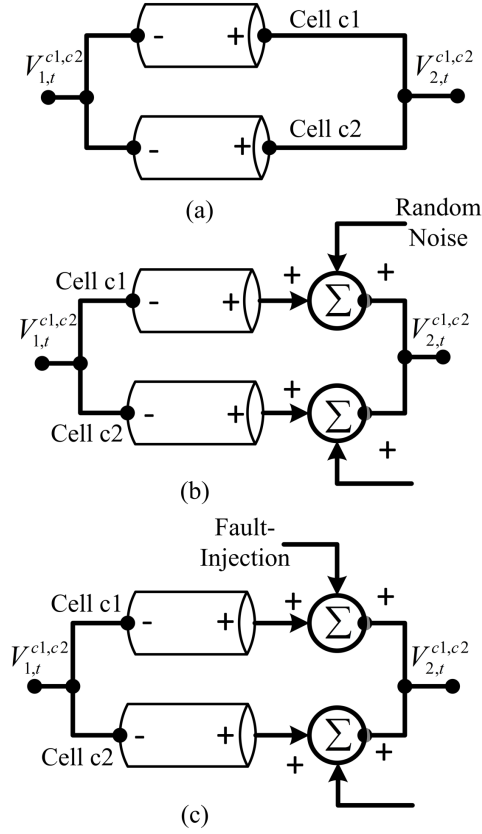
Fig. 2. Cells setup of Li-ion battery pack for current-split estimation: (a) nominal case, (b) with random-noise variance, and (c) with fault-injection

chamber to provide a controlled thermal environment, and a computer used for controlling the current load and supply and data storage through a Labview interface. The noise in the measurements is eliminated with the help of a low-pass filter. The characterization tests and driving cycle test were conducted with a frequency of 10 Hz at 20 ^0C, and the current is considered to be positive at discharge and negative at charge. Note in each test case, Li-ion battery cell measurements of all parameters are given, which can be readily measured by the proposed scheme. However, in this paper, the focus is to estimate the current-split and followed by the voltage.

A. Test Case I: Nominal Current-Split Estimation

The purpose of this study is to examine the estimation capability of the proposed scheme for the current-split of two cells in parallel. The online values of all the parameters of the battery for the two cells are plotted in Fig. 3. It comprises of the sampled current given to two cells, individual current of each cell for testing and verifying our estimation scheme, corresponding voltage profile and temperature during battery charging/discharging operation.

The proposed estimation scheme was implemented to estimate the current-split from the real time measurements of the Li-ion battery cells. This was followed by the calculation of voltage values based on the estimated current-split. Referring to Fig. 4 and 5, the proposed recursive weighted covariance-based filter is used to estimate the respective profiles of current from Cell 1 and Cell 2, respectively. In addition, comparisons with the mainstream Unscented Kalman filter of [33] were made. Referring to Fig. 4 and 5, there is a huge over-shoot spike at the beginning of the measured current in each cell. The proposed filter captured such dynamics more clearly than the regular Unscented Kalman filter. Furthermore, a comparison of MSE and error percentage between the main stream UKF [33], and EKF [31, 32] and the proposed filter is shown in Fig. 6. All the techniques performed reasonably well. However, because of the initialization procedure, the EKF started with a slow time tracking response, causing it to have a higher MSE value in the initial time windows. This is due to the lack in updating the covariance matrix at every iteration, which is not the case for UKF. It performed better than EKF. However, the initial overshoot was not well-captured by the UKF. In contrast, the recursive-based weighted filter was fast enough to capture the dynamics well from the start. Therefore, the proposed method gives more accurate results than EKF UKF as it was able to estimate the deviations of the profile with precision. This is due to its estimating nature using the innovation process used for the initialization.

Referring to Fig.7, the voltage of the circuit has been estimated. This voltage was calculated
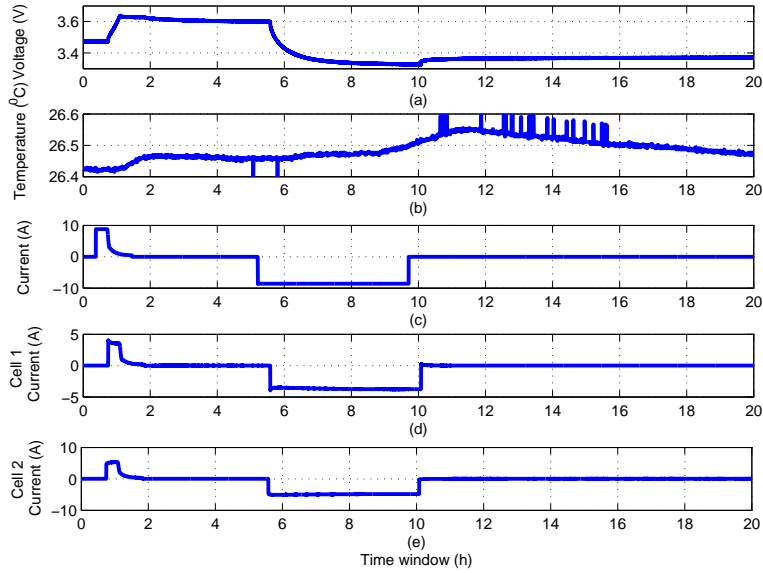
Fig. 3. Test Case I: Li-ion battery cell measurements of the experimental battery pack
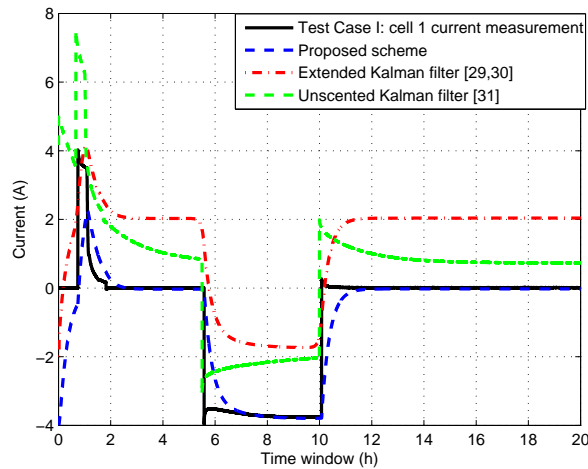
Fig. 4. Test Case I: Comparison of the current estimates of Cell 1

based on the estimation of current-split. The estimation performance with sharp undershoot and overshoots can be seen. The initial dynamics of voltage were being captured well by the regular Unscented Kalman filter. However, UKF was not able to estimate the sharp ramp-down in the voltage profile. This may due to its behavior of tackling singular covariances where trail sets of data are not sufficient in such situations of sharp profiles.
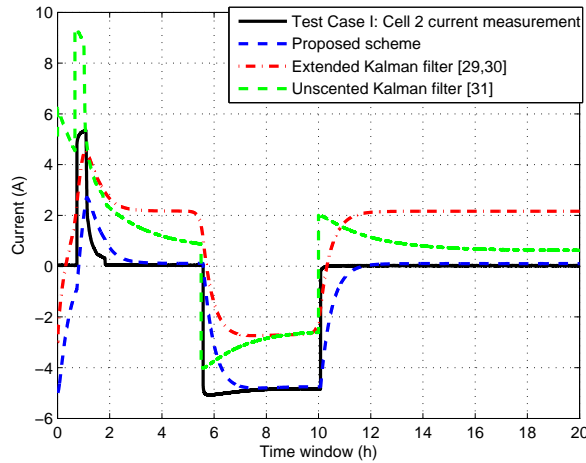
Fig. 5. Test Case I: Comparison of the current estimates of Cell 2
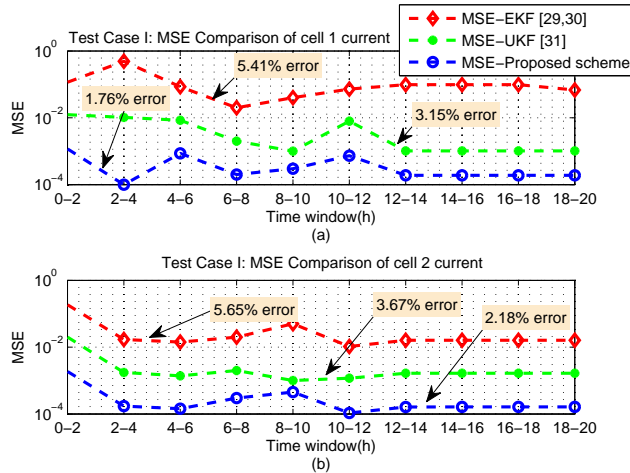
Fig. 6. Test Case I: MSE performance of estimated current for a) Cell 1, and b) Cell 2
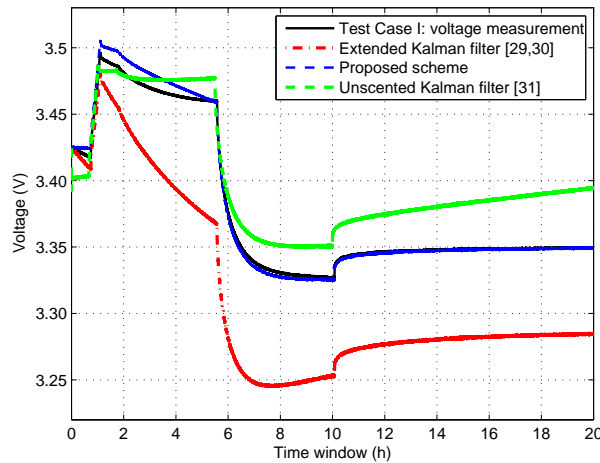
Fig. 7. Test Case I: Estimated voltage of battery cell

B. Test Case II: Current-split Estimation with Random Noise Variance

The objective of this test case is to examine the estimation capacity of the proposed scheme in the presence of random noise variance. The sampled current profile of the parallel circuit and each individual cell, temperature variations, and the corresponding voltage trajectory are shown in Fig. 8. Random noise with a variance between 0.1 and 0.9 was added in the current measurements. Referring to Fig. 9 and 10, the noise variance has introduced some spikes in the current profile. A comparison of the corresponding MSE and percentage error between the main-stream EKF, UKF, and the proposed filter is shown in Fig. 11. In Fig.7, the voltage was estimated. Because of the random noise variance, the voltage dynamics for this case are showing a signature of sinusoid kind of fluctuation. The dynamics of voltage were being captured well by the regular Unscented Kalman filter. Furthermore, a comparison of MSE is shown in Fig. 11. All the schemes performed reasonably well. However, EKF and UKF were not able to estimate the fault thoroughly. EKF may have suffered due to its property of using predefined model for finite difference approximation by calculating Jacobians. Whereas, UKF considers a Gaussian-noise uniformity in the model profile, which was not the case here.

C. Test Case III: Current-split Estimation with Fault-Injection

This test case has been generated to evaluate the performance of the proposed filter in the presence of injected fault. The sampled individual and cumulative current profile can be seen in Fig. 13, followed by profile for temperature variations and voltage. Random faults were injected in the current profile at 6.25–7.5 hours and 10.8–11.75 hours. Fig. 14 and 15 show the current-split profile with fault injection scenarios. The corresponding MSE and percentage error between the main stream EKF, UKF, and the proposed filter is shown in Fig. 16. From these figures, EKF and UKF are not able to estimate the kinks and outliers accurately in the current profiles. Meanwhile, the estimated cumulative voltage outputs are shown in Fig. 17. The same pattern of kinks and
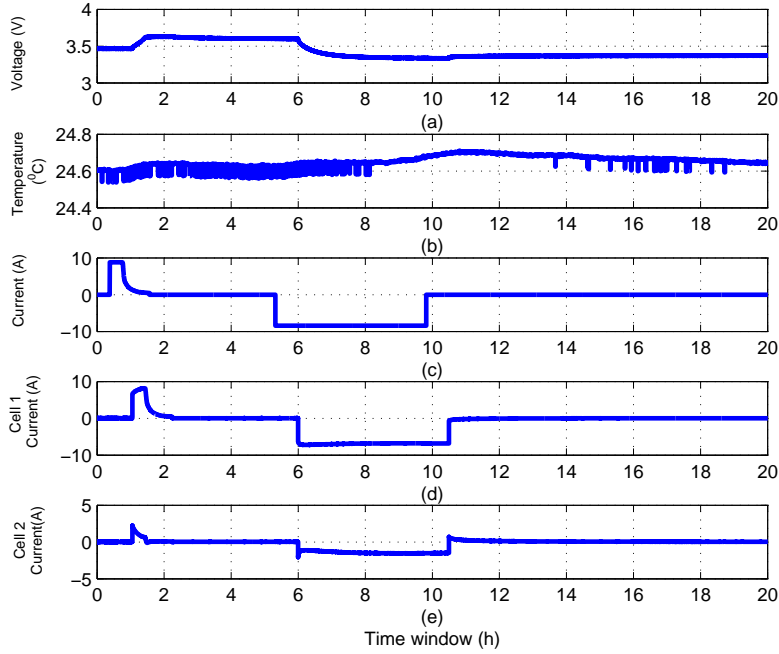
Fig. 8. Test Case II: Li-ion battery cell measurements with random-noise variance

outliers like in Fig. 14 and 15 can also be seen in this profile followed by the estimation analysis.

IV. CONCLUSIONS

The proposed RWEM-based current-split estimation has been effectively demonstrated to estimate current-split against random noise conditions and fault injections. The weighted covariance property of the proposed scheme was incorporated in the initialization of the filter with the innovation process. These enhancements provide more strength to the filter. In the future, an adaptive scheme to estimate the current-split of cells will be proposed to benefit the cell-balancing control of each individual cell to improve the service life of the battery-pack. Moreover, the testing of battery pack cells at different temperatures, varying frequencies and aged cells is one of our high priority agenda for future work.
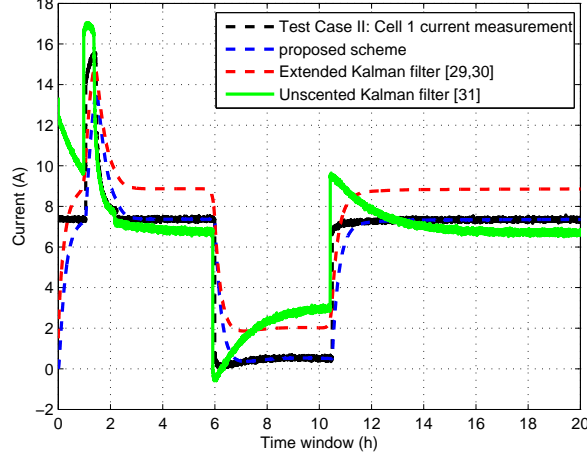
Fig. 9. Test Case II: Comparison of current estimates of Cell 1
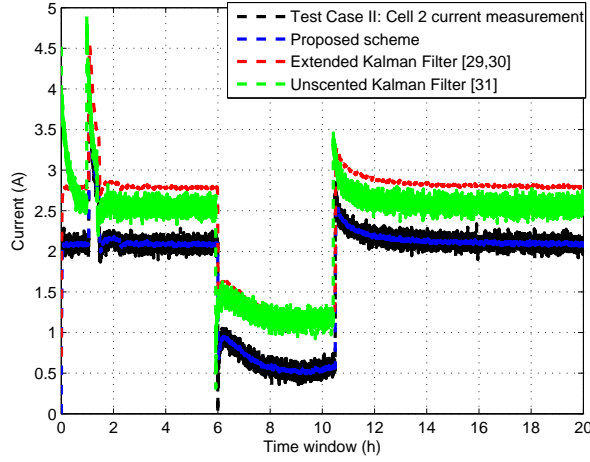
Fig. 10. Test Case II: Comparison of current estimates of Cell 2

APPENDIX

A. Proof of Consistency for (27)

Given the estimate $(\hat{I}_{t|t}^{\mathcal{C}}, P_{t|t}^{\mathcal{C}})$, where $\hat{I}_{t|t}^{\mathcal{C}}$ denotes the estimated current state at time instant t. P refers to the estimated covariance matrix at the respective time instant. For the current-split estimation, let $\tilde{P}_{t|t}^{\mathcal{C}} = (\hat{I}_{t|t}^{\mathcal{C}} - I_{t|t}^{\mathcal{C}})(\hat{I}_{t|t}^{\mathcal{C}} - I_{t|t}^{\mathcal{C}})'$. Then consistency of the covariance is defined as a property that the estimated covariance matrix is no smaller than the true covariance of the
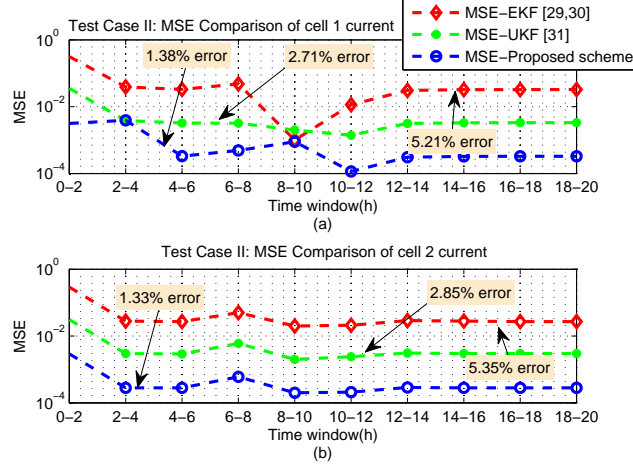
Fig. 11. Test Case II: MSE performance of estimated current of a) Cell 1, and b) Cell 2
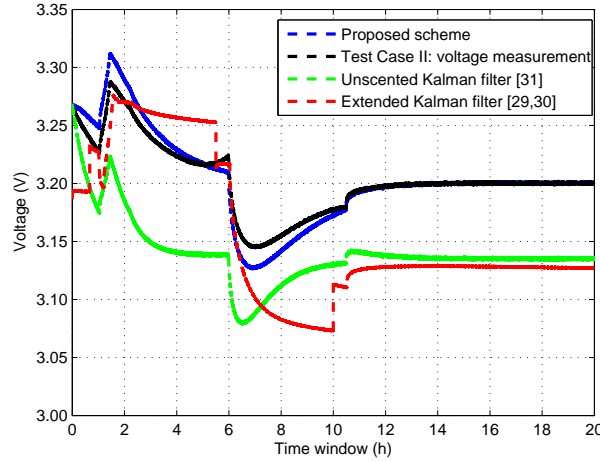
Fig. 12. Test Case II: Voltage estimates of battery cell

estimated state of current.

$$P_{0|0}^{\mathcal{C}} - \tilde{P}_{0|0}^{\mathcal{C}} \geq 0 \tag{34}$$

Considering the definition of (27), the $\tilde{P}_{t|t}^{\mathcal{C}}$ for the current-split is given by:

$$\tilde{P}_{0|0}^{\mathcal{C}} = P_{t|t}^{\mathcal{C}} \sum_{t=0}^{T} A_t^{c1} A_t^{c2} P_{t|t}^{c1^{-1}} \tilde{P}_{t|t}^{\mathcal{C}} P_{t|t}^{c2^{-1}} \geq 0 \tag{35}$$

From (34), the lower bound is as follows:

$$\tilde{P}_{0|0}^{\mathcal{C}} = \sum_{t=0}^{T} A_t^{c1} P_{t|t}^{c2^{-1}} \geq \sum_{t=0}^{T} A_t^{c1} P_{t|t}^{c2^{-1}} \tilde{P}_{t|t}^{c1} P_{t|t}^{c2^{-1}} \tag{36}$$

22

As $A_t^{c2} A_t^{c1} \geq 0$, this follows that:

$$P_{t|t}^{c2^{-1}} \tilde{P}_{t|t}^{c2} P_{t|t}^{c2^{-1}} + P_{t|t}^{c1^{-1}} \tilde{P}_{t|t}^{c1} P_{t|t}^{c1^{-1}} - P_{t|t}^{c2^{-1}} \tilde{P}_{t|t}^{\mathcal{C}'} P_{t|t}^{c1^{-1}} - P_{t|t}^{c1^{-1}}$$

$$\tilde{P}_{t|t}^{\mathcal{C}} P_{t|t}^{c2^{-1}} = \mathbf{E}[(P_{t|t}^{c2^{-1}} \tilde{I}_{t|t}^{c2} - P_{t|t}^{c1^{-1}} \tilde{I}_{t|t}^{c1})(P_{t|t}^{c2^{-1}} \tilde{I}_{t|t}^{c2} - P_{t|t}^{c1^{-1}}$$

$$\tilde{I}_{t|t}^{c1})'] \geq 0 \tag{37}$$

B. Proof of Stability for (33)

Using (33), the discrete Lyapunov equation can be expressed as:

$$M \Omega M' + \Omega = 0 \tag{38}$$

where M' is the conjugate transpose of M. Given that $\Omega > 0$, satisfying (38), if and only if the linear system $I_{t+1}^{\mathcal{C}} = F_t I_t^{\mathcal{C}}$ is asymptotically stable. (33) can be represented in the form of (38), where:

$$M = \lim_{t \to \infty} P_{I,t|t}^{\mathcal{C}} \Big[-(N-1) P_{I,t|t-1}^{\mathcal{C}^{-1}} F_t + P_{I,t|t}^{\mathcal{C}^{-1}} A_{t-1}$$

$$P_{I,t|t}^{\mathcal{C}} A_t^{c1} F_t + P_{I,t|t}^{\mathcal{C}^{-1}} A_{t-1} P_{I,t|t}^{\mathcal{C}} A_t^{c2} F_t \Big], \Omega = W_t R_t W_t',$$

$$W_t = \lim_{t \to \infty} \Big[P_{I,t|t}^{\mathcal{C}} P_{I,t|t}^{\mathcal{C}^{-1}} A_{t-1} P_{I,t|t}^{\mathcal{C}} \Big] (A_t^{c1} + A_t^{c2})$$

REFERENCES

[1] M. Dubarry, B. Y. Liaw, M. S. Chen, S. S. Chyan, K. C. Han, W. T. Sie, and S. H. Wu, "Identifying battery aging mechanisms in large format Li-ion cells," *J. Power Sources*, vol. 196, no. 7, pp. 3420–3425, Apr. 2011.

[2] M. Dubarry, N. Vuillaume, Y. B. Liaw, "Origins and accommodation of cell variations in Li-ion battery pack modeling," *Int. J. Energy Res*, vol. 34, pp. 216–31, Dec. 2009.

[3] K. S. Ng, C.-S. Moo, Y.-P. Chen, and Y-C. Hsieh, "Enhanced coulomb counting method for
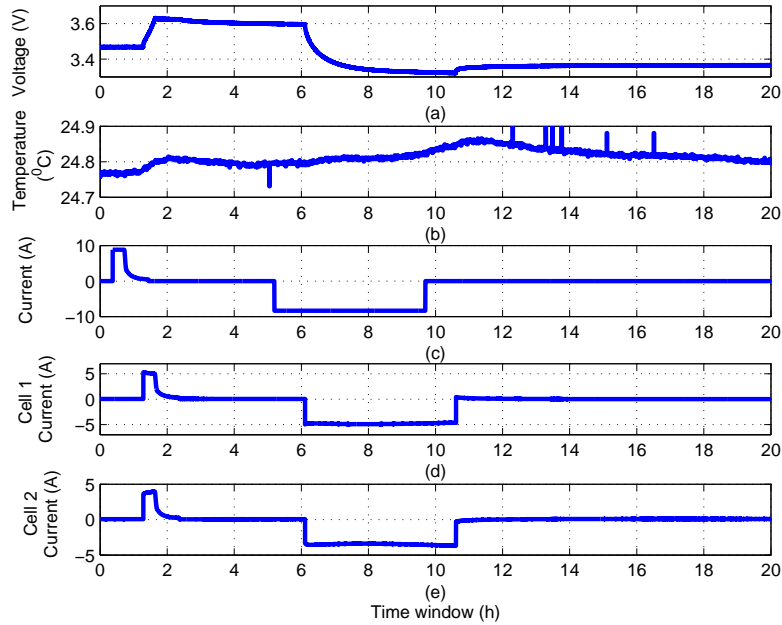
Fig. 13. Test Case III: Li-ion battery cell measurements under fault injections
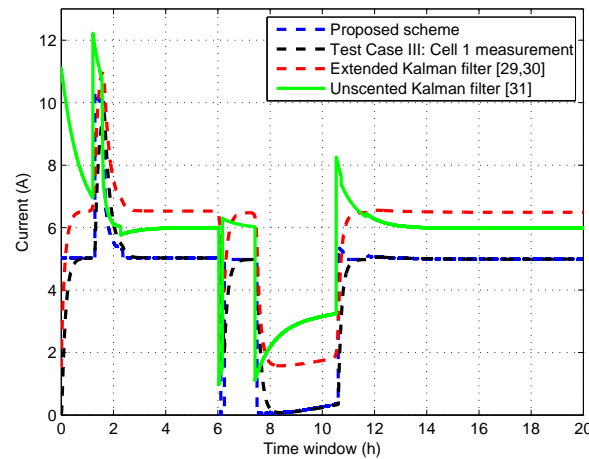
Fig. 14. Test Case III: Comparison of current estimates of Cell 1

estimating state-of-charge and state-of-health of lithium-ion batteries," *Appl. Energy*, vol. 86, no. 9, pp. 1506–1511, Sep. 2009.

[4] Z. Liu, Q. Ahmed, G. Rizzoni, and H. He, "Fault detection and isolation for lithium-ion battery system using structural analysis and sequential residual generation," *7th ASME Annual Dynamic Sys. and Ctrl.*, TX, US, 2014.
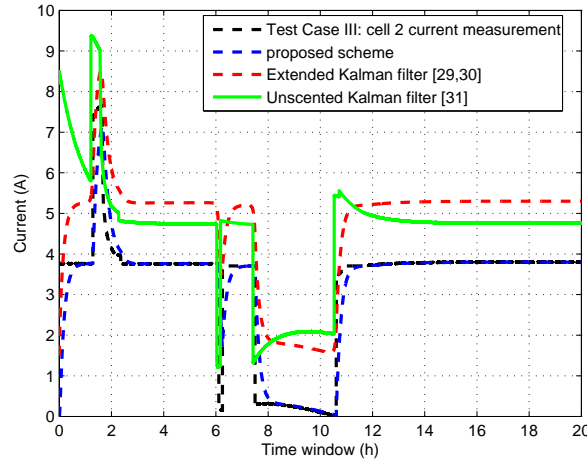
Fig. 15. Test Case III: Comparison of current estimates of Cell 2
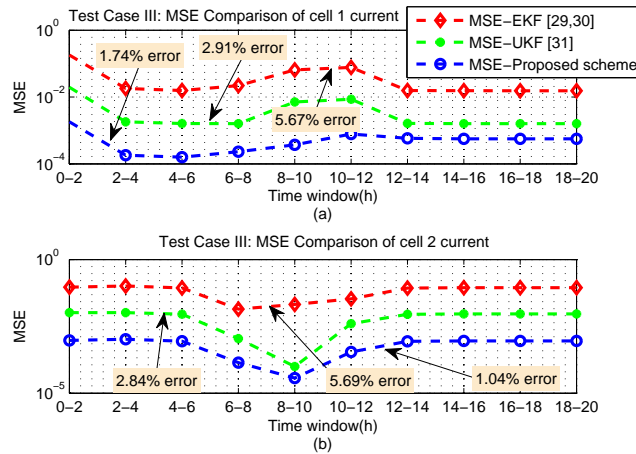
Fig. 16. Test Case III: MSE performance of estimated current of a) Cell 1, and b) Cell 2

[5] Y. Hu, S. Yurkovich, Y. Guezennec, and B. J. Yurkovich, "Electro-thermal battery model identification for automotive applications," *J. Power Sour.*, vol. 196, no. 1, pp. 449-457, Jan. 2011.

[6] J. Marcicki, M. Canova, M., A. T. Conlisk, and G. Rizzoni, "Design and parametrization analysis of a reduced-order electrochemical model of graphite/$LiFePO_4$ cells for SOC/SOH estimation," *Jour. Power Sour.*, vol. 237, pp, 310-324, Sep. 2013.

[7] H. M. Khalid, Q. Ahmed and J. C.-H. Peng, "Health Monitoring of Li-ion battery systems: A median expectation-based diagnosis approach (MEDA)," *IEEE Trans. Transpt. Elec.*, vol. 1, no. 1, pp. 94–105, Jul. 2015.
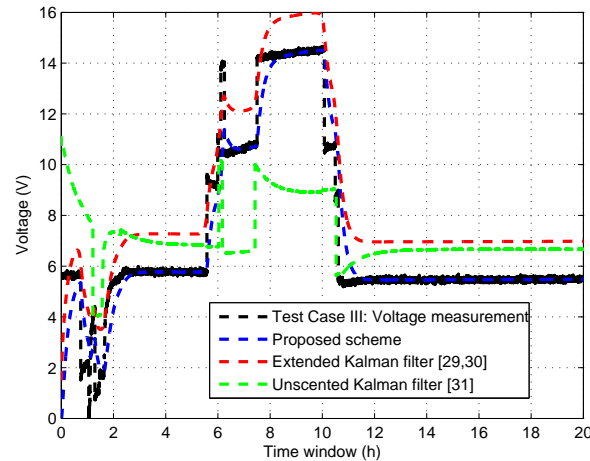
Fig. 17. Test Case III: Voltage estimates of the battery cell

[8] U.S. Department of Energy Vehicle Technologies Program, "Battery test manual for plug-in hybrid electric vehicles," *The Idaho National Laboratory, U.S. Department of Energy National Laboratory, Operated by Battelle Energy Alliance*, revision 3, Sep 2014.

[9] H. Dai, X. Wei, Z. Sun, J. Wang, and W. Gu, "Online cell SOC estimation of Li-ion battery packs using a dual time-scale Kalman filtering for EV applications," *Appl. Energy*, vol. 95, pp. 227–37, Jul. 2012.

[10] J. Wang, Z. Sun, X. Wei, and H. Dai, "Study on the uneven cells problem of the power battery pack in the automotive application by ECM," *Phys. Procedia Part B*, vol. 24, Part-B, pp. 984–96, 2012.

[11] M. Charkhgard, M. Farrokhi, "State-of-charge estimation for lithium-ion batteries using neural networks and EKF," *IEEE Trans. Ind. Elctr.*, vol. 57, pp. 4178–87, Dec. 2010.

[12] K. T. Chau, K. C. Wu, C. C. Chan, "A new battery capacity indicator for lithium-ion battery powered electric vehicles using adaptive neuro-fuzzy inference system," *Energy Convers. Mngmt.*, vol. 45, no. 11-12, pp. 16811692, Jul. 2004.

[13] T. Hansen, C. J. Wang, "Support vector based battery state of charge estimator," *J Power Sources*, vol. 141, no. pp. 351–358, Mar. 2005.

[14] Q. S. Shi, C. H. Zhang, N. X. Cui, "Estimation of battery state-of-charge using v-support vector regression algorithm," *Int. J. Automot. Tech.*, vol. 9, no. 6, pp. 759–64, Dec. 2008.

[15] D. Andre, C. Appel, T. Soczka-Guth, D. U. Sauer, "Advanced mathematical methods of SOC and SOH estimation for lithium-ion batteries," *J. P. Sources*, vol. 224, pp. 2027, Feb. 2013.

[16] H. Dai, X. Wei, Z. Sun, "State and parameter estimation of a HEV Li-ion battery pack using adaptive Kalman filter with a new SOCOCV concept," *Proc. IEEE Int. Conf. meas. tech. mechatr. autom.*, pp. 375–380, Apr. 2009.

[17] G. L. Plett, "Extended Kalman filtering for battery management systems of LiPB-based HEV battery packs- Part 3: State and parameter estimation," *J. Power Sources*, vol. 134, pp. 277292, 2004.

[18] G. L. Plett, "Extended Kalman filtering for battery management systems of LiPBbased HEV battery packs- Part 2: Modeling and identification," *J. Power Sources*, vol. 134, no. 2, pp. 262–276, Aug. 2004.

[19] J. Y. Han, D. C. Kim, M. Sunwoo, "State-of-charge estimation of lead-acid batteries using an adaptive extended Kalman filter," *J. Power Sources*, vol. 188, no. 2, pp. 606–612, Mar. 2009.

[20] F. Sun, X. Hu, Y. Zou, S. Li, "Adaptive unscented Kalman filtering for state of charge estimation of a lithium-ion battery for electric vehicles," *Energy*, vol. 36, no. 5, pp. 3531–40, May 2011.

[21] G. L. Plett, "Sigma-point Kalman filtering for battery management systems of LiPB-based HEV battery packs: Part 1: Introduction and state estimation," *J. Power Sources*, vol. 161, no. 2, pp. 1356–68, Oct. 2006.

[22] S. Santhanagopalan, and R. E. White, "State of charge estimation using an unscented filter for high power lithium ion cells," *Int. J. Energy Res.*, vol. 34, pp. 152–63, Dec. 2009.

[23] S. Schwunk, N. Armbruster, S. Straub, J. Kehl, M. Vetter, "Particle filter for state of charge

and state of health estimation for lithiumiron phosphate batteries," *J. Power Sources*, vol. 239, pp. 705–10, Oct. 2013.

[24] Y. He, X. Liu, C. Zhang, Z. Chen, "A new model for State-of-Charge (SOC) estimation for high-power Li-ion batteries," *Appl. Energy*, vol. 101, pp. 808–814, Jan. 2013.

[25] K. J. Astrom, and R. M. Murray, "Feedback systems: An introduction for scientists and engineers," *Princeton University Press*, 2008.

[26] A. C.-Arenas, S. Onori, G. Rizzoni, "A control-oriented lithium-ion battery pack model for plug-in hybrid electric vehicle cycle-life studies and system design with consideration of health management," *J. Power Sources*, vol. 279, pp. 791–808, Apr. 2015.

[27] "Standard handbook for electrical engineers," by H. W. Beaty (Editor), and D. G. Fink (Editor), Aug. 2012.

[28] Y. Hu, S. Yurkovich, Y. Guezennec, and B. J. Yurkovich, "Electro-thermal battery model identification for automotive applications," *J. Power Sour.*, vol. 196, no. 1, pp. 449-457, Jan. 2011.

[29] J. Marcicki, M. Canova, M., A. T. Conlisk, and G. Rizzoni, "Design and parametrization analysis of a reduced-order electrochemical model of graphite/$LiFePO_4$ cells for SOC/SOH estimation," *J. Power Sour.*, vol. 237, pp, 310-324, Sep. 2013.

[30] "Battery test manual for Plug-In hybrid electric vehicles," *U.S. Dept. Ener. Vehicle Tech. Program*, Revision 0, Mar. 2008.

[31] A. Singh, A. Izadian, and S. Anwar, "Adaptive nonlinear model-based fault diagnosis of Li-ion Batteries," *IEEE Trans. Indus. Elect.*, Article in Press, vol. 62, no. 2, pp. 1002–1011, Jul. 2014.

[32] H. He, R. Xiong, X. Zhang, F. Sun, and J. Fan, "State-of-Charge estimation of the lithium-ion battery using an adaptive extended Kalman filter based on an improved Thevenin model,"

IEEE Trans. Vehi. Tech., vol. 60, no. 4, pp. 1461–1469, May 2011.

[33] H. Hea, R. Xiong, and J. Peng, "Real-time estimation of battery state-of-charge with unscented Kalman filter and RTOS μCOS-II platform," *Applied Energy*, Article in Press, DOI:10.1016/j.apenergy.2015.01.120.